Journal of Solid State Chemistry **149,** 49–55 (2000)
Article ID jssc.1999.8493, available online at http://www.idealibrary.com on IDEAL®

Preparation, Structure, and Magnetic Studies of a New $Sr_{11}Re_4O_{24}$ Double Oxide

K. G. Bramnik,* G. Miehe,* H. Ehrenberg,*,† H. Fuess,* A. M. Abakumov,‡ R. V. Shpanchenko,‡ V. Yu. Pomjakushin,§ and A. M. Balagurov§

*Department of Materials Science, University of Technology Darmstadt, D-64287, Darmstadt, Germany; †Interdisciplinary Research Centre in Superconductivity, Cambridge, CB3 OHE, United Kingdom; ‡Department of Chemistry, Moscow State University, 119899 Moscow, Russia; and §Laboratory of Neutron Physics, JINR, 141980 Dubna, Russia

Received December 15, 1998; in revised form August 23, 1999; accepted September 7, 1999

DEDICATED TO PROFESSOR DR. HEINZ DIETER LUTZ ON THE OCCASION OF HIS 65TH BIRTHDAY

The complex oxide $Sr_{11}Re_4O_{24}$ has been synthesized and its crystal structure was determined by a combination of X-ray powder analysis (space group $I4_1/a$; $a = 11.6779(1)$ Å, $c = 16.1488(2)$ Å; $Z = 4$) and electron diffraction. Refinement of the crystal structure was carried out using neutron powder diffraction data ($\chi^2 = 1.85$). The compound has a cation-deficient perovskite-related structure where cation vacancies are located at the A-sublattice. Re and Sr atoms occupy B-positions in an ordered "rock-salt" manner. The perovskite framework is strongly distorted due to rotation of ReO_6 octahedra, leading to a formation of the eightfold coordination for Sr atoms in B-positions. An ordered arrangement of Re^{+6} and Re^{+7} cations is proposed on the basis of different average Re–O distances. The $Sr_{11}Re_4O_{24}$ structure could be considered as a $Ca_{11}Re_4O_{24}$ type of perovskite structure distortion. A magnetic order of $Sr_{11}Re_4O_{24}$ (ferro- or ferrimagnetic) is observed from SQUID measurements ($T_C = 12.0$ K). A moment of $\mu = 0.80\,\mu_B$ is derived from the paramagnetic region (30–200 K) for Re^{6+}.

INTRODUCTION

At present, only a few double oxides of alkaline earth metals and low valence Re have been reported in the literature and only few structures are well characterized. Several compounds found in the systems comprising alkaline-earth and rhenium oxides with Re in formal oxidation state between +6 and +7 have perovskite-derived structures. These structure types exhibit numerous lattice distortions dependent on the type of cations in A- and B-sublattices. The $M_2Re_2O_9$ (M = Ba, Sr) (1,2) oxides have hexagonal perovskite-like structures based on a $9R(chh)_3$ close-packed stacking of the MO_3 layers where Re atoms are situated in the octahedral interstices. Units of three face-sharing octahedra, of which the middle octahedron contains a cation vacancy to overcome the electrostatic repulsion between highly charged neighboring Re^{+6} cations, are linked by corner-sharing and form infinite chains along the [001] direction. The $M_5Re_2O_{12}$ (M = Ca, Sr) (3) oxides with Re in formal oxidation state +7 have also a hexagonal perovskite-like structure, where Re and M atoms have a distorted octahedral oxygen coordination, $d_{(Re-O)} = 1.80$–1.97 Å, the remaining alkaline earth atoms form eight- and nine-fold polyhedra. The Ca_3ReO_6 compound (4) belongs to the $A_2BB'O_6$ (Ca_2CaReO_6) perovskites with a "rock-salt" type distribution of Re and Ca atoms over the B-cation sublattice. The ReO_6 and CaO_6 octahedra are cooperatively tilted with respect to $a^+b^-b^-$ Glazer notation (5). The tilt and distortion of octahedra together with B-cation ordering decrease the symmetry from orthorhombic to monoclinic with an angle close to 90°, as it was shown by Woodward (6) on the base of a topological analysis of the tilting distortions for ordered $A_2BB'O_6$ perovskites. The recently reported $Ca_{11}Re_4O_{24}$ compound (7) has a perovskite-distorted structure too.

In the present investigation we describe the synthesis, crystal structure, and magnetic properties of a new $Sr_{11}Re_4O_{24}$ compound.

EXPERIMENTAL

SrO and ReO_3 (STREM Chemicals, 99.9%) oxides were chosen as starting materials. SrO was obtained by decomposition of $SrCO_3$ at 1100°C for 24 h in air. Three moles of SrO and 1 mol of ReO_3 were intimately mixed, ground in an agate mortar, pressed into 0.5-g pellets, and placed in alumina boats to avoid reaction with the silica tube during annealing. The samples were sealed in silica tubes with 8–10 cm^3 volume at atmospheric pressure in air. The pellets were annealed at 800°C for 48 h. Finally all samples were cooled in a furnace.

0022-4596/00 $35.00

X-ray diffraction data for phase analysis and crystal structure determination were collected using a STADI/P powder diffractometer ($CuK\alpha_1$ radiation, curved Ge monochromator, transmission mode, step 0.02° (2θ), PSD counter). The structure solution was made using integral intensities with a CSD program package (8). The final X-ray powder crystal structure refinement was carried out by the RIETAN-97 program (9). The Rietveld method with a modified pseudo-Voigt profile function was used for the final refinement.

Neutron diffraction experiment was performed at the temperature 10 K with the high-resolution Fourier diffractometer (HRFD) at the IBR-2 pulsed reactor in Dubna.

The electron diffraction (ED) investigations were performed on a Philips CM20 UT transmission electron microscope, operating at an accelerating voltage of 200 kV.

The magnetic properties of $Sr_{11}Re_4O_{24}$ have been studied with a superconducting quantum interference device (SQUID) from Quantum Design in the temperature range from 1.8 to 200 K and field strength up to 5 T.

RESULTS AND DISCUSSION

(*a*) *Structure Determination*

The X-ray diffraction pattern of an annealed sample with Sr_3ReO_6 bulk composition was almost completely indexed on the base of a body-centered tetragonal cell with $a = 11.6779(1)$ Å and $c = 16.1488(2)$ Å. The indexing of the X-ray diffraction pattern was confirmed by electron diffraction study. The preliminary electron diffraction study did not reveal any superstructural spots corresponding to the symmetry decrease or unit cell expansion. Since the reflections with hkl: $h + k + l = 2n + 1$, $hk0$: $h,k = 2n + 1$, and $00l$: $l = 4n + 1$ were systematically absent, space group $I4_1/a$ was proposed for further crystal structure computation.

The integral intensities of the reflections from the angular range 5–70° were determined by profile fitting and used for the calculation of three-dimensional Patterson distribution. Their analysis revealed the positions of Re and a part of Sr atoms. The atomic coordinates of the other Sr and oxygen

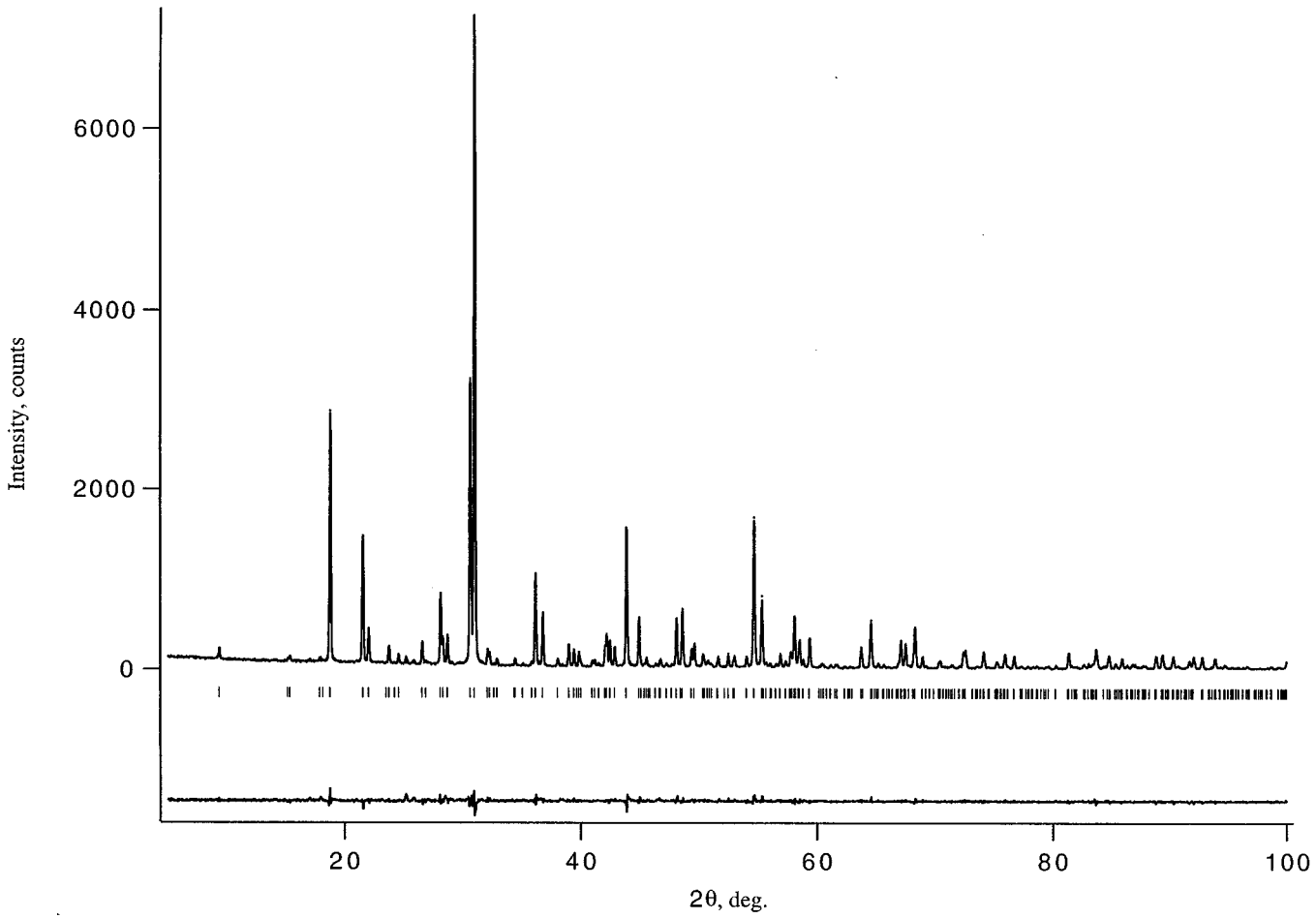

FIG. 1. Experimental, calculated, and difference X-ray patterns for $Sr_{11}Re_4O_{24}$.

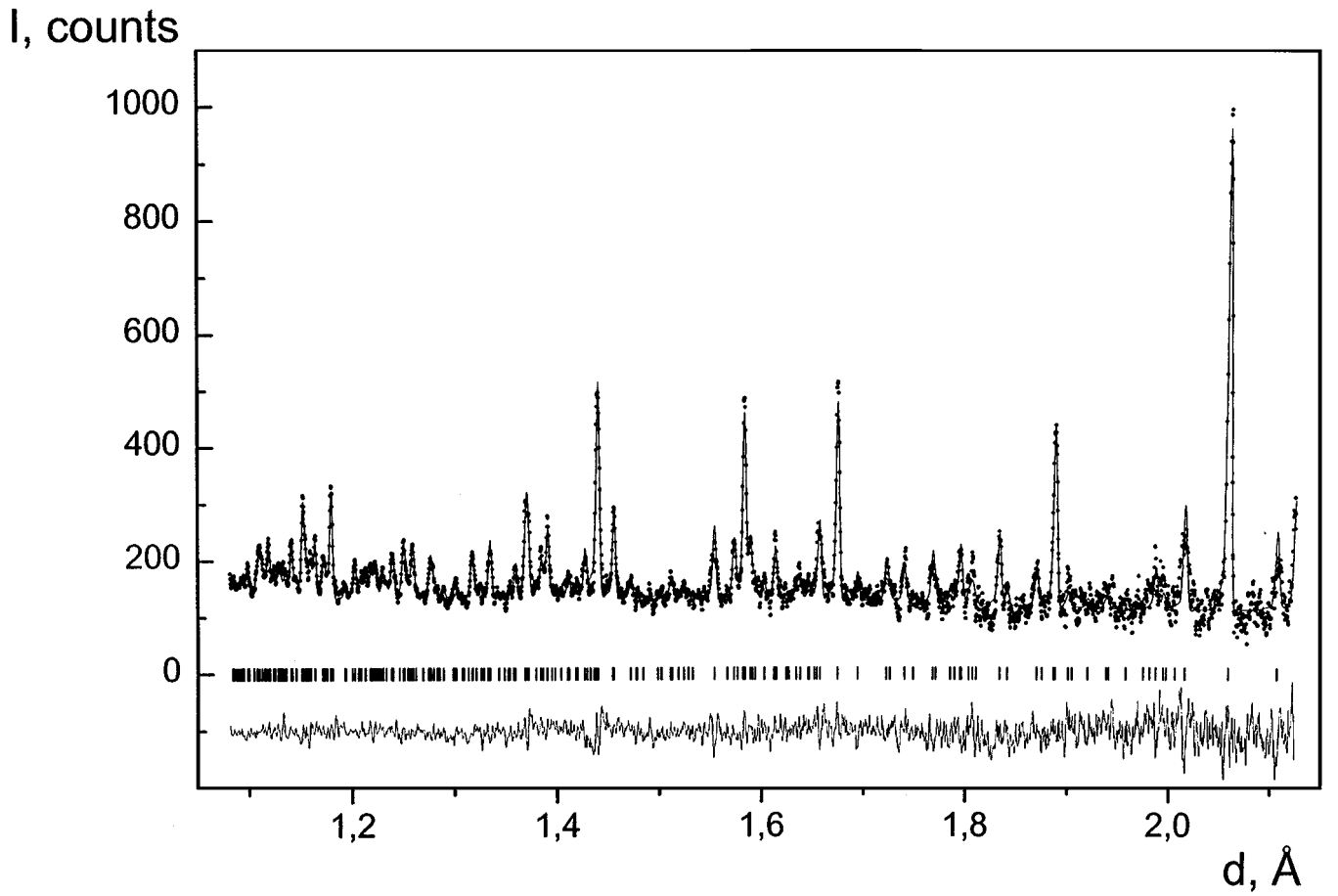

FIG. 2. Experimental, calculated, and difference neutron diffraction patterns for $Sr_{11}Re_4O_{24}$.

atoms were found by a sequence of Fourier and difference Fourier syntheses. Prior to the refinement the impurity peaks were removed from the raw data by profile analysis since they did not overlap with the peaks from the main phase. After sequential iterations good agreement between experimental and calculated patterns was achieved: $R_I = 0.011$, $R_P = 0.056$, $R_{wP} = 0.079$. The observed, calculated, and difference X-ray diffraction patterns are shown in Fig. 1. Then the neutron powder diffraction investigation was performed to prove the obtained structure model of $Sr_{11}Re_4O_{24}$ compound. The final refinement was carried out with the fixed thermal parameters 0.5 $Å^2$ for the Sr and Re atoms and 1 $Å^2$ for the oxygen ones. It shows very good agreement with the X-ray powder diffraction data refinement ($\chi^2 = 1.85$). The composition of the compound determined from structure refinement differs from the bulk composition of the sample and corresponds to the formula $Sr_{2.75}ReO_6$ ($Sr_{11}Re_4O_{24}$). The observed, calculated, and difference neutron diffraction patterns are shown in Fig. 2. The crystallographic parameters, positional parameters and the main interatomic distances for $Sr_{11}Re_4O_{24}$ are listed in Tables 1, 2, and 3, respectively.

The cell parameters of $Sr_{11}Re_4O_{24}$ are clearly connected with the parameters of the perovskite subcell a_{per}: $a = 2\sqrt{2}\,a_{per}$, $c = 4a_{per}$. Formally the $Sr_{11}Re_4O_{24}$ formula can be written as $Sr_7\square(Sr_4Re_4)O_{24}$, which allows us to consider this compound as a cation-deficient perovskite with vacancies in the A sublattice. Two projections of the $Sr_{11}Re_4O_{24}$ crystal structure along [001] and [110] axes

TABLE 1
Crystallographic Parameters for $Sr_{11}Re_4O_{24}$

Space group	$I4_1/a$
a (Å)	11.6779(1)
c (Å)	16.1488(2)
Cell volume ($Å^3$)	2202.26(5)
Z	4
Calculated density (g/cm^3)	6.312
2θ range (time/step)	5–100°, 60 s
No. of reflections	564
Refinable parameters	54
Reliability factors	$R_I = 0.011$, $R_P = 0.056$, $R_{wP} = 0.079$

TABLE 2
Positional and Thermal Parameters for $Sr_{11}Re_4O_{24}$ from Neutron Diffraction Data

Atom	x/a	y/b	z/c	B (Å^2)
Sr(1)	0	1/4	1/8	1
Sr(2)	1/2	1/4	0.6175(8)	1
Sr(3)	0.2068(2)	− 0.0131(8)	− 0.1399(6)	1
Sr(4)	0.2126(7)	0.2324(8)	0.5311(5)	1
Re(1)	0	0	0	1
Re(2)	0	0	1/2	1
O(1)	0.8607(9)	0.126(1)	0.2712(5)	0.5
O(2)	0.628(1)	0.1363(8)	0.2479(6)	0.5
O(3)	0.2790(8)	0.235(1)	0.3667(5)	0.5
O(4)	0.829(1)	0.171(1)	0.6657(6)	0.5
O(5)	0.9045(8)	0.125(1)	0.4774(6)	0.5
O(6)	0.3148(9)	0.1435(9)	0.6759(7)	0.5

are shown in Figs. 2a and 2b, respectively. Figure 2a shows that Re and Sr(4) atoms both occupy the B-position of the perovskite subcell in an ordered manner, forming a "rock salt" type cation sublattice. The remaining Sr atoms are placed in the channels of a three-dimensional framework formed by ReO_6 and $Sr(4)O_8$ polyhedra connected by corner-sharing and edge-sharing. Re(1) and Re(2) atoms are located in distorted octahedra ($d_{Re(1)-O} = 1.92$–1.97 Å, $d_{Re(2)-O} = 1.87$–1.88 Å). Since the octahedral coordination is not typical for Sr cations, the perovskite octahedral framework is significantly transformed. So, $Re(1)O_6$ octahedra are only slightly tilted along [110], whereas $Re(2)O_6$ ones are rotated along the same axis by $\approx 45°$. This changes the Sr(4) oxygen environment from an octahedron to an irregular 8-fold polyhedron where Sr(4)–O distances vary in the range of 2.32–2.87 Å. As a result the $Re(2)O_6$ octahedron is edge-shared by the equatorial oxygen atoms O(4) and O(6) to four $Sr(4)O_8$ polyhedra and connected with two $Sr(4)O_8$

TABLE 3
Main Interatomic Distances (Å) for $Sr_{11}Re_4O_{24}$ from Neutron Diffraction Data

Sr(1)–O(1)	3.21(2) × 4	Sr(4)–O(1)	2.65(2) × 1
Sr(1)–O(2)	2.86(2) × 4	Sr(4)–O(2)	2.45(2) × 1
Sr(1)–O(3)	2.59(1) × 4	Sr(4)–O(3)	2.76(1) × 1
Sr(2)–O(1)	2.67(2) × 2	Sr(4)–O(4)	2.50(1) × 1
Sr(2)–O(2)	2.73(2) × 2		2.52(1) × 1
Sr(2)–O(3)	3.26(1) × 2	Sr(4)–O(5)	2.32(1) × 1
Sr(2)–O(5)	2.55(1) × 2	Sr(4)–O(6)	2.82(2) × 1
Sr(2)–O(6)	2.67(1) × 2		2.87(1) × 1
Sr(3)–O(1)	2.62(2) × 1	Re(1)–O(1)	1.97(2) × 2
	2.59(2) × 1	Re(1)–O(2)	1.95(2) × 2
Sr(3)–O(2)	2.84(2) × 1	Re(1)–O(3)	1.92(1) × 2
	2.97(2) × 1	Re(2)–O(4)	1.88(1) × 2
Sr(3)–O(3)	2.62(1) × 1	Re(2)–O(5)	1.87(1) × 2
	2.60(1) × 1	Re(2)–O(6)	1.88(1) × 2
Sr(3)–O(4)	2.61(1) × 1		
Sr(3)–O(5)	2.59(1) × 1		
Sr(3)–O(6)	2.50(1) × 1		

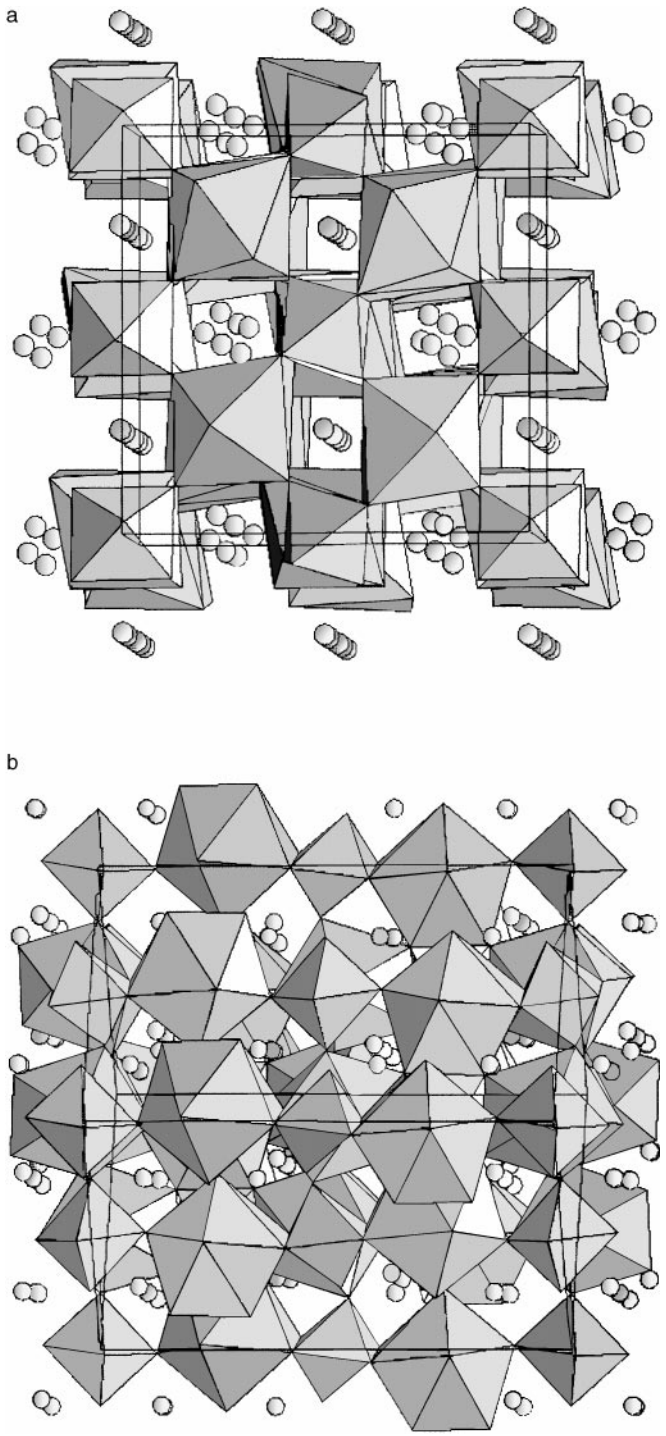

FIG. 3. The projections of $Sr_{11}Re_4O_{24}$ crystal structure along [001] (a) and [110] (b).

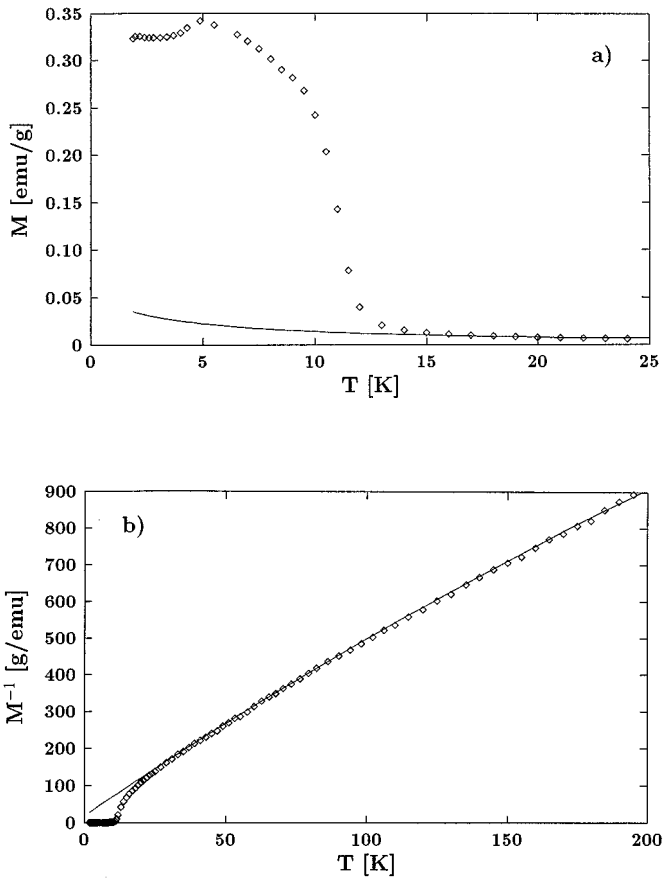

FIG. 4. Temperature dependence of magnetization (a) and its inverse (b) of $Sr_{11}Re_4O_{24}$ at constant field strength of 0.25 T.

ones by corner-sharing via the apical oxygen atoms O(5) (Fig. 2b). Re(1)O_6 octahedra are linked with the Sr(4) polyhedra only by corner sharing. The rotation of ReO_6 octahedra leads to an appearance of two kinds of nonequivalent channels filled by A-cations (Fig. 2a). In the first one only 3/4 of A-positions are occupied by Sr(1) and Sr(2) cations with 12-fold ($d_{Sr(1)-O} = 2.59$–3.21 Å) and 10-fold ($d_{Sr(2)-O} = 2.55$–3.26 Å) coordinations, respectively. The second one contains Sr(3) atoms surrounded by eight oxygen atoms ($d_{Sr(3)-O} = 2.50$–2.97 Å).

The formal oxidation state of Re calculated from the refined composition is equal to $+6.5$. The Re atoms in the $Sr_{11}Re_4O_{24}$ structure are distributed over two nonequivalent positions and we can expect an ordered placement of Re^{+6} and Re^{+7} cations. The reasonable argument for this ordering is the nonnegligible difference between average Re–O distances for Re(1)O_6 ($\langle d_{Re-O}\rangle = 1.95$ Å) and Re(2)O_6 ($\langle d_{Re-O}\rangle = 1.88$ Å) octahedra. These interatomic distances are in very good agreement with the ionic radii of Re^{+6} and Re^{+7} cations for octahedral coordination: $r(Re^{+6}) = 0.52$ Å (9), $r(Re^{+7}) = 0.49$ Å (3). It should be noted that we did not use the radius $r(Re^{+7}) = 0.57$ Å proposed by Shannon (10) since it was obtained from only one compound, $Re_2O_7 \times 2H_2O$, with one highly distorted octahedral site, where the Re–O distances vary between 1.65 and 2.16 Å. Certainly, the average value for this radius 0.49 Å, calculated from $Ca_5Re_2O_{12}$ and $Sr_5Re_2O_{12}$ structures (3), looks more reliable than the value given by Shannon. Consequently, we can propose that the Re(1) position is preferentially occupied by Re^{+6} cations, whereas Re^{+7} ones are placed in the Re(2) site.

The composition $Sr_{11}Re_4O_{24}$ ($Sr_{2.75}ReO_6$) is close to Sr_3ReO_6. An increase of the size of strontium atoms in comparison with calcium ones in Ca_3ReO_6 results in essential structural rearrangement in anion framework and a formation of vacancies in the A-sublattice. The type of polyhedra sharing is different for these two structures in spite of similar B-cation "rock-salt" arrangement. In most cases the octahedral tilting distortion of the perovskite structure leads to a change of the first coordination sphere around A-cations. At the same time, the coordination environment of B-cations remains almost unchanged. The main reason for this distortion is the requirement to optimize the distances between A-cations and oxygen atoms. The geometrical relationship between A–O and B–O distances is determined by the Goldschmidt factor. In contrast the degree of octahedra tilting in the $Sr_{11}Re_4O_{24}$ structure significantly exceeds the usual tilt angles (which are approximately equal to 10°) and leads to dramatic changes in the first coordination sphere for half of the B-cations. This structural transformation is caused by the large size of Sr cations, which have to be surrounded by more than six oxygen atoms.

(*b*) *Magnetic Properties of the $Sr_{11}Re_4O_{24}$*

$Sr_{11}Re_4O_{24}$ orders ferro- or ferrimagnetically below the Curie temperature of $T_C = 12(1)$ K as deduced from the temperature dependence of magnetization at constant field strength of 0.25 T (see Fig. 3). A Curie–Weiss law, modified by an additional temperature independent contribution M_O,

$$M(T) = \frac{C}{T - \Theta} + M_0, \qquad [1]$$

was fitted to the data from 30 to 200 K, revealing $M_0 = 1.65 \times 10^{-4}$ emu/g, $\Theta = -3.5$ K, and a paramagnetic moment of 0.80 μ_B per Re^{+6} ion, which belong to the very rare case of $5d^1$ electron configuration. In a crystal field of octahedral symmetry the orbital levels split into a doublet and a low-lying triplet. The Landé factor g for the latter is zero, and a not-vanishing value for the magnetic moment is due only to a crystal field of lower symmetry and contributions from the doublet for a finite value of crystal field

TABLE 4
The Field Dependence of Magnetization at Different Temperatures below T_C for $Sr_{11}Re_4O_{24}$

T(K)	α (10^{-6}emu/(gG))	H_0(G)	σ(G)	H_C(G)	$\int_{loop} MdH$ ((emu G)/g)	$M_{H\to 0}(\mu_B$ per Re(+6)-ion)
5.0	4.082	93860	9900	257	10910	0.0718
6.5	4.224	86700	6630	246	7030	0.0686
7.5	4.361	79950	4450	198	4585	0.0654
8.4	4.575	71010	2500	183	2485	0.0609
9.3	4.871	59930	975	~60	~810	0.0547
10.0	5.521	45710	~260	~12	~195	0.0473

splitting (11). A quantitative analysis of these effects must be based on the anisotropy of the g tensor and requires a single crystal.

The field dependence of magnetization was measured at different temperatures below T_C (see Fig. 4 for $T = 5$ and 10 K). Starting from saturation the magnetization decreases linearly with field, followed by a pronounced kink and smoothly joining into linear behavior for saturation in opposite field direction. The field dependence can be described by

$$M(H) = M_1(H) + M_2(H), \qquad [2]$$

with

$$M_1(H) = \begin{cases} \alpha(H + H_0), & H \text{ decreasing} \\ \alpha(H - H_0), & H \text{ increasing} \end{cases} \qquad [3]$$

and

$$M_2(H) = \begin{cases} 2\alpha H_0 \tanh[(H + H_C)/\sigma], & H \text{ decreasing and } H < -H_C, \\ 2\alpha H_0 \tanh[(H - H_C)/\sigma], & H \text{ increasing and } H > H_C, \\ 0, & \text{else}, \end{cases} \qquad [4]$$

Four parameters, α, H_0, σ, and H_C, have to fitted to the observed data points. The results are given in Table 4, and the calculated hysteresis loops are shown in Fig. 4 as drawn lines. The agreement is excellent for $T = 5$ to 8.4 K, but at 9.3 K slight deviations can be seen in the field range approaching saturation, more pronounced at 10 K. The areas within one complete loop are calculated according to

$$\int_{loop} MdH = 4\alpha H_0(H_C + \sigma \ln 2) \qquad [5]$$

and given in Table 4, too. The remnant magnetization provides precise values for the temperature dependence of the resulting ferromagnetic moment. Based on molecular field approximation for a spin-half system,

$$\frac{\mu(T)}{\mu_0} = \tanh \frac{\mu(T)/\mu_0}{T/T_C} \qquad [6]$$

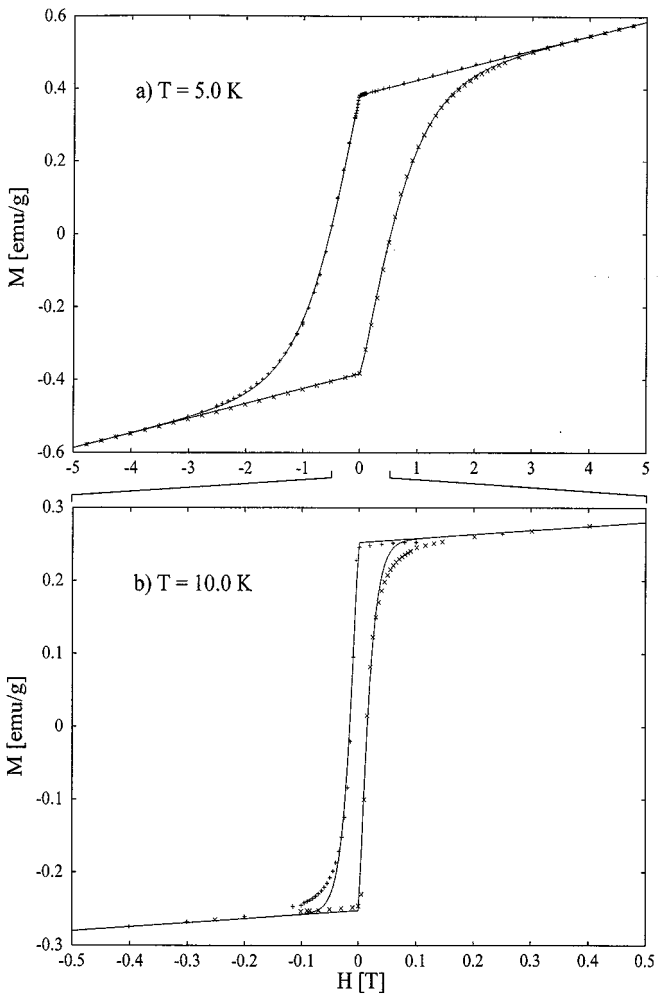

FIG. 5. Hysteresis loops of $Sr_{11}Re_4O_{24}$ at 5.0 K (a) and 10.0 K (b).

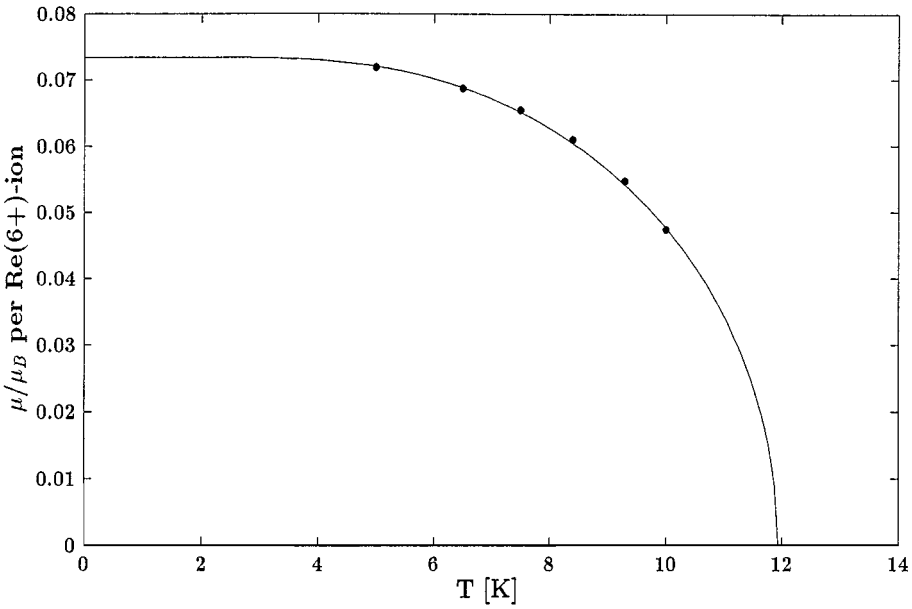

FIG. 6. Observed and calculated temperature dependence of spontaneous magnetization.

gives $\mu_0 = 0.0734\mu_B$ per Re(+ 6) ion and $T_C = 11.94$ K (see Fig. 5). This small value of μ_0 as compared to the paramagnetic moment of 0.8 μ_B indicates weak ferrimagnetism in $Sr_{11}Re_4O_{24}$ at low temperature (see Fig. 6).

ACKNOWLEDGMENTS

This work was supported by BMBF (Bundesministerium fuer Bildung und Forschung). A. Abakumov and R. Shpanchenko are grateful to Russian Science Foundation (Grant 97-03-33432a) for financial support.

REFERENCES

1. B. L. Chamberland and F. C. Hubbard, *J. Solid State Chem.* **26,** 79 (1978).
2. C. Calvo, H. N. Ng, and B. L. Chamberland, *Inorg. Chem.* **17,** 699 (1978).
3. H. A. Mons, M. S. Schriewer, and W. Jeitschko, *J. Solid State Chem.* **99,** 149 (1992).
4. A. M. Abakumov, R. V. Shpanchenko, and E. V. Antipov, O. I. Lebedev, and G. Van Tendeloo, *J. Solid State Chem.* **131,** 305 (1997).
5. A. M. Glazer, *Acta Crystallogr. B* **28,** 3384 (1972).
6. P. M. Woodward, *Acta Crystallogr. B* **53,** 32 (1997).
7. W. Jeitschko, H. A. Mons, U.Ch. Rodewald, and M. H. Möller, *Z. Naturforsch.* **53b,** 31 (1998).
8. L. G. Akselrud, Yu.N. Grin, P.Yu. Zavalij, V. K. Pecharsky, and V. S. Fundamentsky, Thes. report on 12-th ECM, p. 155, Moscow, 1989.
9. F. Izumi, *in* "The Rietveld Method" (R. A. Young, Ed.), Chap. 13. Oxford Univ. Press, Oxford, 1993.
10. R. D. Shannon and C. T. Prewitt, *Acta Crystallogr. B* **25,** 925 (1969).
11. A. Abragam and B. Bleaney, "Electron Paramagnetic Resonance of Transition Ions," Chap. 7. Oxford Univ. Press, Oxford, 1970.